ACS APPLIED MATERIALS & INTERFACES

Research Article

www.acsami.org

High Performance and Long-Term Stability in Ambiently Fabricated Segmented Solid-State Polymer Electrochromic Displays

Julian Remmele,*[,†] D. Eric Shen,[‡,§] Tero Mustonen,[‡] and Norbert Fruehauf[†]

[†]Institute for Large Area Microelectronics, University of Stuttgart, 70569 Stuttgart, Germany

[‡]BASF SE, 67056 Ludwigshafen, Germany

Supporting Information

ABSTRACT: This work reports on the performance of a segmented polymer electrochromic display that was fabricated with solution-based processes in ambient atmosphere. An encapsulation process and the combination of structured wells for the polymer electrochrome and electrolyte layers as well as the use of a preoxidized counter polymer yields high contrasts and fast switching speeds. Asymmetric driving—with respect to time—of the display is investigated for the first time and the degradation effects in the electrochrome layer are analyzed and addressed to yield a stable device exceeding 100 000 switching cycles. A printed circuit board was integrated with the display, allowing the device to be run as a clock, where the segments only required short pulses to switch without the need for a constant current to maintain its state. Such an application pairs well with the advantages of electrochromic polymers, drawing on its high contrast, stability, and ability to maintain its colored or colorless state without the need for a constant power supply, to demonstrate the promise as well as the challenges of developing more sophisticated electrochromic devices.

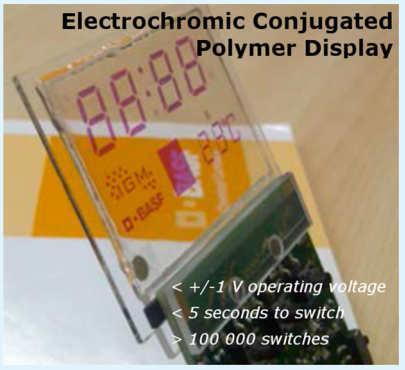

KEYWORDS: *solid-state device, electrochromic, stability, segmented, ambient processing*

1. INTRODUCTION

In the last 5 years, there have been many advances in the field of organic electrochromic polymers (ECPs) that have brought the technology closer to realization. A complete color palette of high-contrast and fast-switching soluble conjugated polymers has been synthesized, and the ability to blend these colors to access virtually any color has been demonstrated.[1−3] A minimally color changing polymer has also been synthesized that can serve as the frontplane counter electrode in a device with minimal effect on the color of the active layer.[4] It has been demonstrated that the power and energy requirements needed to perform a complete switch are low and can be driven by other organic electronic devices, making ECPs potentially capable of integration into all-organic flexible devices.[5] The processing of electrochromic films and devices using roll-to-roll compatible techniques has recently been demonstrated.[6,7] Finally, it has been shown that after applying UV and oxygen barrier layers to ECP films and devices, the operational lifetimes can be greatly extended, and for some colors are comparable to the stabilities achieved in inorganic materials, which have traditionally held an advantage in this area.[8,9] With these advances, ECPs are poised to offer faster-switching and higher-contrast films than their inorganic or small-molecule counterparts in virtually any color, as well as possessing lower power and energy consumption, and the necessary stability after encapsulation for a wide range of applications. Most of the organic-soluble ECP-based devices constructed up to this point in the literature have been small lab-scale window devices, which can be easily fabricated and evaluated, with one notable exception demonstrating large area device switching.[10] However, given the many recent advances, the next step is to begin incorporating ECPs into more sophisticated devices to demonstrate their feasibility in a wide range of applications.

Segmented displays[11−13] have been demonstrated for use in simple low-power information type displays as well as active-matrix displays for use in applications such as electronic readers.[14−16] While there is no need to structure the electrochromic layer in window-type devices, structuring of the active material must be introduced when working with displays comprised of segments, pixels or logos. So far, device patterning has been predominantly carried out by inkjet printing,[17,18] coating through a shadow mask,[19] or flexographic printing.[20] A variety of techniques exist to pattern electrodes and contacts, and several specifically for electrochromic displays (ECDs) have been reviewed.[21]

In this work, a high performance segmented electrochromic clock display was fabricated. PProDOT-$(CH_2OEtHx)_2$ (first synthesized by Reeves et al.[22]), which is magenta colored in its neutral state and colorless in its oxidized state, was used as the electrochromic polymer. This material has been widely employed as the ECP in ECDs, due to its high contrast, millisecond switching speeds between fully colored and fully colorless states and robust switching stability.[23] For optimal device operation, a balanced amount of charges must be

Received: March 9, 2015
Accepted: May 15, 2015
Published: May 15, 2015

DOI: 10.1021/acsami.5b02090
ACS Appl. Mater. Interfaces 2015, 7, 12001−12008

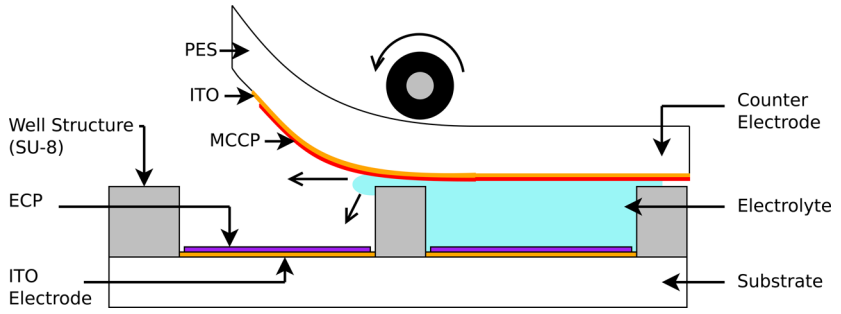

Figure 1. Principal structure of assembled devices and lamination of the counter electrode.

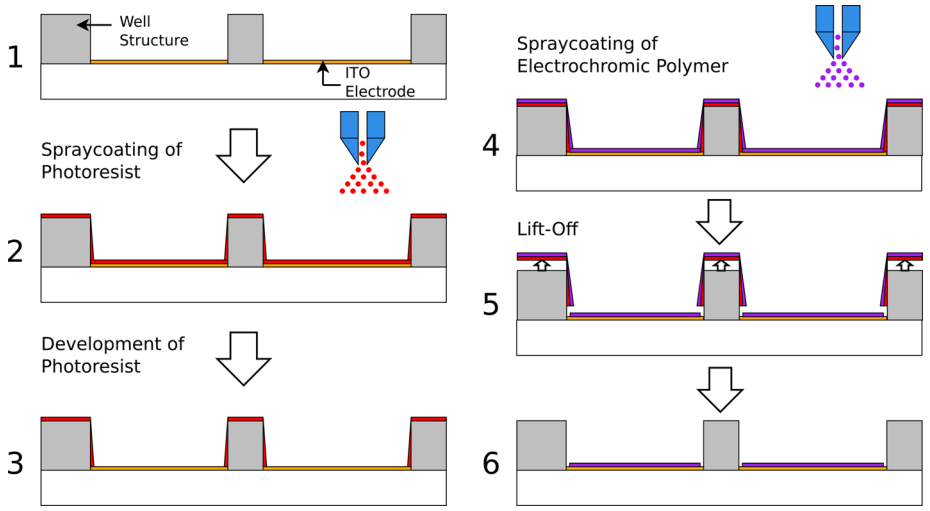

Figure 2. Lift-off process: (2) Spray coating of (1) original substrate and (3) development of the photoresist, followed by (4) spray coating of the ECP and (5) lift off yields (6) the finished substrate. Dimensions are not to scale: the height of the well is 15 μm, whereas its width is several millimeters.

exchanged at the working electrode as well as at the counter electrode. A minimally color changing polymer (MCCP) based on poly(3,4-propylenedioxypyrrole) (PProDOP-C_{18}) that is spray-processable, very stable over thousands of switches, and allows switching the ECP in the order of seconds while being almost colorless in the visible range was developed as the charge storage layer.[4] The individual segments of a displays are defined through the use of substrates with structured wells formed on substrates before coating the ECP, thus permitting a variety of film-coating or printing techniques. Additionally, the device thickness can be precisely defined, and crosstalk between segments can be controlled. A number of concerns unique to segmented displays not encountered in window-type devices will be explored, such as the need to structure the back electrode. Finally, a clock demonstrator was assembled to illustrate the contrasts and the lifetimes achievable in a structured system. Although very high lifetimes have already been achieved with numerical displays, this was done using a liquid electrolyte filled by capillary forces and an electrochemically polymerized material.[24] With the methods presented in this work, we were able to build the first structured polymer electrochromic device using ambient, solution-based processes yielding an all-solid state device and achieving lifetimes of greater than 200 000 switching cycles.

2. RESULTS AND DISCUSSION

2.1. Process. Figure 1 illustrates the setup of our electrochromic display, as well as the architecture and layers present in our device. For electrochromic display-type applications other than electrochromic windows, there will be the need to structure the electrochromic layer as well as the electrode (ITO) to obtain individual segments, pixels or logos. Because the ECP material used here is conductive in its transparent oxidized state, it is not possible to pattern only the ITO layer, as charges between transparent and colored magenta segments would rapidly and uncontrollably equilibrate, leading to partially colored states in both segments.

As mentioned before, structuring of the ECP is usually carried out through various printing techniques. A drawback of inkjet printing with our ECP is that formulation of the appropriate ink to achieve high quality films (homogeneous and optically dense) is nontrivial. In contrast, spray-coating using a simple airbrush gun is a technique which reproducibly deposits homogeneous and optically dense films over a wide range of spraying parameters, such as variations in spraying pressure, spray gun distance from substrate, and sweep rate, to name a few. Additionally, it is a technique that can be adapted to large scale roll-to-roll processes and spray coating yields porous layers, which is ideal for adequate electrolyte penetration.[25] To structure spray-coated films, we paired the coating technique with a lift off process (see Figure 2): before the ECP is applied, the desired pattern is defined through the use of wells. These wells were made from SU-8, a transparent epoxy-based negative-tone photoresist with a high aspect ratio that is chemically resistant when cured. Next, a negative tone photoresist is spray-coated over both the SU-8 wells as well

DOI: 10.1021/acsami.5b02090
ACS Appl. Mater. Interfaces 2015, 7, 12001−12008

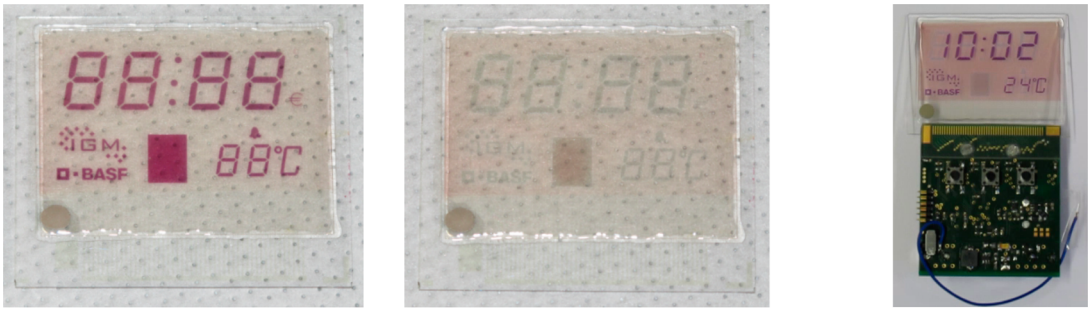

Figure 3. Display fabricated in this work (a) in its colored, magenta state; (b) in its colorless, transparent state; and (c) mounted to demonstrator PCB. The demonstrator uses a microcontroller (and additional driving circuitry) to run a clock, show the current temperature and logos of the partners involved in this work.

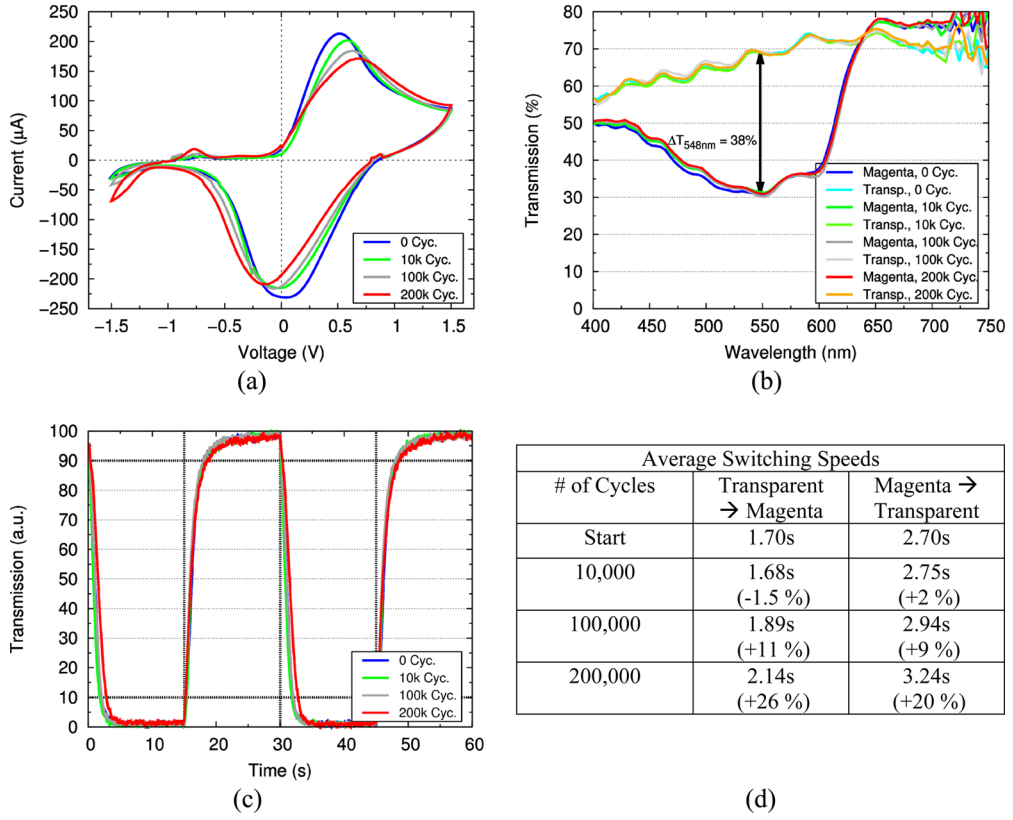

Average Switching Speeds		
# of Cycles	Transparent → Magenta	Magenta → Transparent
Start	1.70s	2.70s
10,000	1.68s (-1.5 %)	2.75s (+2 %)
100,000	1.89s (+11 %)	2.94s (+9 %)
200,000	2.14s (+26 %)	3.24s (+20 %)

Figure 4. (a) CV (scan rate: 0.1 V/s), (b) spectra (referenced to air), and (c, d) switching speed measurements for a symmetrically (0.15 Hz cycle frequency, at +0.8 V and −0.4 V) driven EC display measured at λ_{max} (548 nm): initially and at 10 000, 100 000, and 200 000 cycles. The CV measurement is done for the complete display while transmission measurements are from an individual seven-segment. Measurements in c are normalized to be comparable and values in d are the time to reach 90% of a full switch averaged over 4 segments on two different devices. The used voltages are the same as during cycling.

as the ITO layer, followed by developing the photoresist, leaving photoresist on the walls of the wells, while exposing the ITO layer. After structuring of the photoresist, the ECP is sprayed onto the substrate. Finally, the photoresist is removed in an acetone ultrasonic bath, thereby also removing the ECP on the SU-8 wells and only leaving the patterned magenta ECP.

The ECP itself is not soluble in acetone and therefore the patterned segments should not be removed during this process. Nevertheless, the mechanical stress of the ultrasonic bath can cause the ECP to be partially removed when immersed too long. We therefore limited the time in the ultrasonic bath to a few seconds (<15 s). To examine the effects on the ECP during this process, we reviewed spectra of the displays before and after the lift off and found that the change in transmittance is less than 3% at 540 nm (see Figure S1 in the Supporting Information). This demonstrates that the ultrasonic bath has a minimal impact on the ECP layer and this structuring procedure minimizes the stress endured by the ECP.

In addition to assisting in the structuring of the ECP layer, wells made from SU-8 afford several additional advantages to device performance. The SU-8 wells also serve to embed the electrolyte for each display segment and to act as a passivation layer for the underlying ITO tracks leading to the individual segments. This prevented leakage of the electrolyte from the

DOI: 10.1021/acsami.5b02090
ACS Appl. Mater. Interfaces 2015, 7, 12001−12008

segments and device failure due to degradation and/or decomposition of the ITO. Furthermore, in the assembled device the SU-8 layer is also used to define a uniform and small electrolyte layer thickness in the electrochemical cells. Thickness control has been shown to have an effect on the performance of electrochemical devices, with thinner electrolyte layers leading to the highest device contrasts.[26] This is especially important when employing a flexible substrate, such as the polyether sulfone (PES) front plane, which would otherwise have a tendency to bend and deform, leading to inhomogeneous thicknesses throughout the device. Although transparent spacers have been used in LC displays to define precise device thicknesses, here the SU-8 wells are able to perform that role while simultaneously affording other advantages to the performance of the device.

Device assembly was accomplished through lamination of the front and backplanes, followed by UV-curing of the electrolyte. Lamination is a key step not only for assembling the device but also for depositing the electrolyte layer into the defined segments. During electrolyte loading, due to poor wetting of the SU-8 (hydrophobic) by the electrolyte (hydrophilic), there is a tendency for the electrolyte to be repelled from the edges of the wells, leading to the formation of droplets within the wells. This makes alternative processes such as blade coating or printing of the electrolyte unsuitable. Instead, this was overcome by using an excess of electrolyte in conjunction with lamination, a process that forces the electrolyte into wells while simultaneously pressing out the excess electrolyte. Additionally, this leads to the presence of a thin electrolyte on top of the SU-8 layer which, after UV-curing, helps to adhere the device together. In general, UV-curable electrolytes have ionic conductivities below 1 mS/cm,[27] and at thicknesses at over 1 mm can often produce unwanted optical effects. In particular, thick layers of our electrolyte become a translucent yellow solid. However, for the small electrolyte thicknesses employed here, after UV-curing the electrolyte was transparent and colorless, as can be seen in Figure 3. UV-curing of our electrolyte could be completed in 1 min, or under white light over the course of hours, with no noticeable degradation occurring to the ECP or MCCP layers. This illustrates that the lamination and UV-curing steps offer a simple route toward device assembly that can readily be incorporated into a high-throughput roll to roll process.

2.2. Performance. The as-fabricated display is shown in its colored and colorless states (compare Figure 3a, b), where the color saturation and the colorlessness in the two states are readily apparent; additionally, the device was highly transmissive because of the thin electrolyte layer and the good optical transparency of the substrates. The devices were quantitatively evaluated based on their electrochemical, spectroelectrochemical, and kinetic switching speed performance. Switching times are stated for 90% of a full switch. An emphasis was placed on examining the long-term stability of the device by switching the segments for up to 200 000 cycles between the colored and colorless states. The performance of the segments was reevaluated after 10 000, 25 000, 100 000, and 200 000 cycles. All optical measurements are taken at one of the seven-segments comprising each numerical display visible in Figure 3, whereas the cyclic voltammetry (CV) is taken from switching all segments of the display simultaneously.

Figure 4 shows the result of the above-mentioned tests, demonstrating complete switching of the device when symmetrically cycled (for 3.3s in each state) between a narrow voltage window of +0,8 V (colorless, $L^* = 89$, $a^* = 1$, $b^* = 7$) and −0,4 V (colored, $L^* = 70$, $a^* = 22$, $b^* = -7$). These properties are preserved even after 200 000 cycles. The narrow voltage window, rapid switching, and device stability are due to several factors. First, both ECP and MCCP are polymers that themselves have low oxidation potentials that directly contribute to the low operational voltages. Second, the charge-balanced magenta and MCCP layers allow the magenta segments to rapidly achieve a full switch. Finally, the preoxidation of the MCCP layer prior to device assembly leads to a device with both electrodes already in its appropriately charged state. It is possible to assemble the device with both magenta and MCCP in their neutral "as-sprayed" state, but then overpotentials are needed to "break in" the device, leading to overoxidation and poorer device stabilities.

In the device CV, two main peaks related to the electrochromic redox switching of the device are observed at approximately +0.6 V and −0.1 V (compare Figure 4a). At potentials beyond this, other peaks are observed. Switching at these larger potentials was found to degrade the material and lower the display's contrast when cycled continuously. In choosing a voltage window to switch the device, a trade-off is made between more rapid switching at larger potential windows but higher stability at narrower potential windows. The voltages used for testing were chosen at slight overpotentials beyond the observed redox peaks.

The device CV and spectroelectrochemistry in Figure 4a, b offer additional insight into the stability of the device. After 200 000 cycles, no discernible change in the absorption of the oxidized or reduced states is visible (minimal deviations can be attributed to placing each segment in a slightly different position in the spectrophotometer beam for each measurement). Throughout the 200 000 cycles, the contrast of the entire device (i.e., measuring also the substrate, electrolyte, etc.) is maintained at $\Delta T = 38\%$ at λ_{max} (548 nm) and $L^*a^*b^*$ coordinates remain almost the same (colorless: $L^* = 89$, $a^* = 1$, $b^* = 7$ and colored: $L^* = 70$, $a^* = 21$, $b^* = -9$). Looking at the device CV, a drop in current and a shift in the position of the main redox peaks is clearly noticeable over the course of 200 000 switches. This suggests the redox process is becoming more irreversible, although the onset of the redox peaks remains unchanged. Curiously, secondary peaks at −ca. −0.8 V and ca. −1.5 V in the CV emerge with repeated cycling. This is unexpected, as these potentials are outside the potential window used to stress test the device. During repeated cycling, we qualitatively observed that the smaller elements (e.g., logos, colon) of the display seem to visually degrade faster during cycling, whereas larger elements (e.g., seven-segments) are stable throughout all 200 000 cycles. The progression of the degradation can also be observed in microscopic images of the ECP layer. In smaller segments (see Figure S2 in the Supporting Information), this effect is very visible, but negligible for larger segments. We also relate the evolution of the CV curves to these degradations, as with increasing numbers of cycles it becomes more difficult to insert charges into these elements of the display, making the process less reversible. The reason for the faster degradation of the smaller elements is unknown at this point and needs further study, but most likely stems from inefficient charge consumption as described by other groups.[7,28]

Although no degradation is visible in the spectroelectrochemistry of the larger elements, their switching speed

DOI: 10.1021/acsami.5b02090
ACS Appl. Mater. Interfaces 2015, 7, 12001−12008

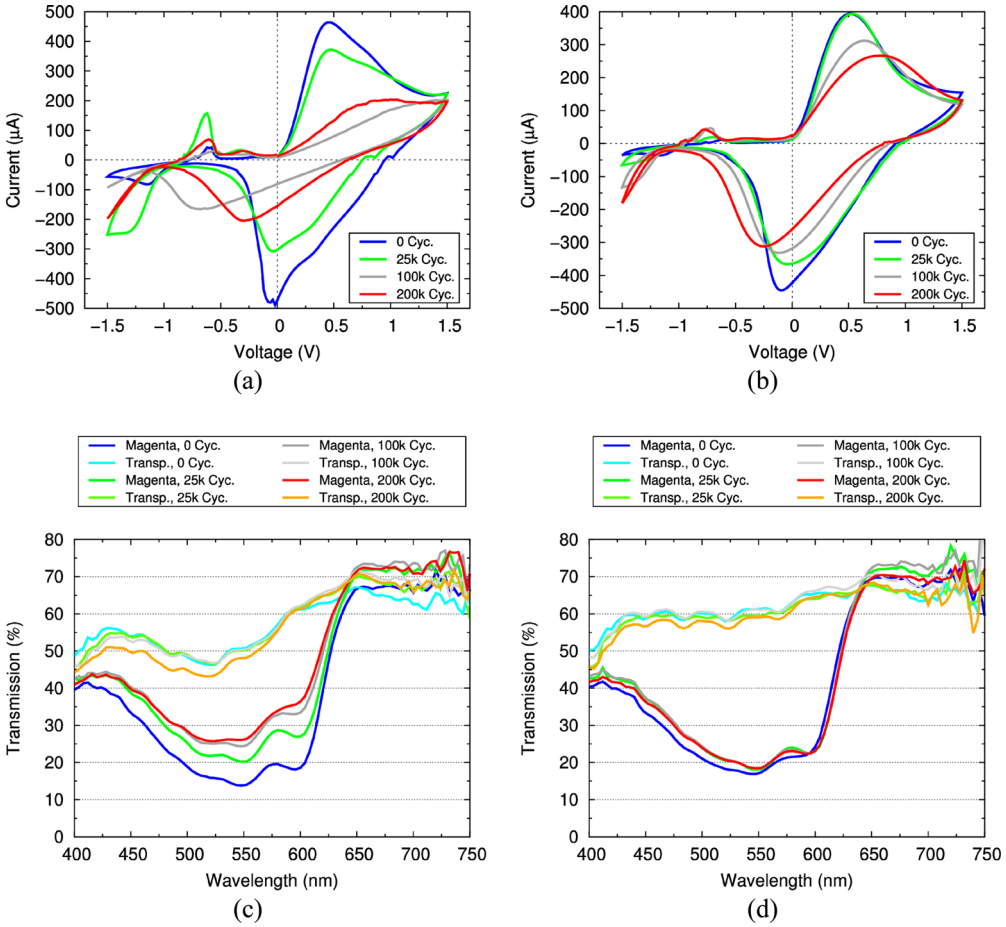

Figure 5. (a, b) CV (scan rate: 0.1 V/s) and (c, d) spectra for asymmetrically switched devices ((a, c) 6.6 s transparent, 3.3 s magenta; (b, d) 3.3 s transparent, 6.6 s magenta). The CV measurements are done for the complete display, whereas transmission measurements are from individual seven-segments.

decreases slightly over 200 000 cycles, as summarized in Figure 4d. After 10 000 cycles, the change in switching speed is within the margin of error of the measurement, whereas after 100 000 cycles the switching times increase by approximately 10%, up to an increase of more than 20% for 200 000 cycles with respect to the initial state. This occurs simultaneously with the trend in the device CVs over 200 000 cycles. As the redox peaks become more irreversible with increasing numbers of cycles, they also gradually drift outside of the applied voltage window of device switching, which leads to slower device kinetics. Increasing the potential window to encompass the redox peaks leads to faster switching, but at the expense of device stability. Nevertheless, the switching times even after 200 000 cycles are fast enough for full switching to be realized within the 3.3 s per switch.

These results illustrate high long-term stability for symmetrically driven devices built with the presented process, which motivated us to test how the device performed as a clock (compare Figure 3c). A driver printed circuit board (PCB) was attached which updates the clock, temperature and other display elements once every minute. This is done by applying ±1.1 V for 3 s to the individual segments followed by 57 s without a voltage applied. The application of a larger voltage window stems from the driver chip's limitation to a minimum voltage interval of 2.2 V. The ability to run the display in this fashion highlights an advantage of ECPs, which can remain in their oxidized or neutral states for a period of time after the applied voltage has been removed, thus lowering power consumption. When running displays in this demonstrator, again certain segments degrade faster than others. As the segments fail, the switching speed becomes progressively slower until the segment no longer switches. One likely reason for this is the larger potential window applied to drive the clock. A second possibility is also the asymmetric switching of each segment, where segments are no longer switched at regular intervals between the colored and colorless states. For example, the upper right element of the seven-segment displaying single minutes is driven to its transparent state two times every 10 min—at numbers 5 and 6— whereas it is driven to its colored magenta state for all other numbers, i.e., eight times every 10 min.

As seen in Figure 3c, the regions of the display outside of the Magenta segments develop a pink hue over time. This hue arises from a partially oxidized MCCP layer. Although the MCCP backplane is fully oxidized and colorless prior to assembly, over time the film discharges. This is not an issue for the MCCP segments in the region across from the magenta segments, which undergo full charging and discharging as the clock updates, and as a result regions like the rectangle in the middle of the device are able to achieve a more colorless hue during switching. One possible solution then would be to segment the MCCP backplane as well to remove the extraneous counter electrode material and the unwanted coloration. We attempted to segment the MCCP backplane

DOI: 10.1021/acsami.5b02090
ACS Appl. Mater. Interfaces 2015, 7, 12001−12008

as well, however, this was unsuccessful as the device stability was worse for these devices.

To better understand the effects of asymmetric switching on device stability, we assembled devices and switched them asymmetrically for 3.3 s in one state and 6.6 s in the other state. Figure 5 shows the results of these tests where we demonstrate two cases of asymmetric switching. It is quite noticeable that applying a voltage of +0.8 V for 6.6 s (transparent state) and a voltage of −0.4 V for 3.3 s (magenta state) degrades the devices very fast, whereas in the opposite case we observe a much less pronounced degradation. To begin with, we discuss the case of rapid degradation. The colored state deteriorates heavily over 200 000 cycles, increasing about 13% in transmission (see Figure 5c). This can again be observed in microscopic pictures of the ECP layer with degradation effects similar to those mentioned before (compare Figure S2 in the Supporting Information). The device CV (see Figure 5a) also illustrate this behavior: as mentioned before, secondary peaks at −0.8 and −1.5 V increase dramatically over 200 000 cycles while the main redox peaks decrease rapidly in intensity, especially after 100 000 cycles. In addition, the secondary peaks seem to degrade again at 200 000 cycles as well. Compared to the initial state, the switching times increase on average by more than 30, 120, and 200% after 25 000, 100 000, and 200 000 cycles, respectively (see Figure S3a, c in the Supporting Information).

For the inverse asymmetric drive, applying a voltage of +0.8 V for 3.3 s and a voltage of −0.4 V for 6.6 s, the degradation is not as pronounced. Although smaller elements (e.g., colon) degrade as before, the ECP layer of larger elements (e.g., seven-segment) shows little change in its spectroelectrochemistry over 200 000 cycles, as shown in Figure 5d, where the magenta state increases by 1.5% and transparent state decreases by 2% in transmission over 200 000 cycles. Microscope images of ECP films of these asymmetrically driven devices show slightly more signs of degradation compared to the symmetrically switched devices. In the device CV, we again observe the redox peaks drifting apart and decreasing in intensity, with increasing number of switches. Switching times increase, but not as dramatically as for the other asymmetrically driven device. Although there is almost no change after 25 000 cycles, larger increases in switching times by around 30 and 65% on average are observed at 100 000 and 200 000 cycles, respectively (see Figure S3b, d in the Supporting Information). From these results, symmetric driving of the device leads to the most stable devices, while between the two asymmetrically driven devices, the most severe device failure is observed when the device is held in the colorless state at +0.8 V for 6.6 s and in the colored state at −0.4 V for 3.3 s. This seems to suggest that driving the device into the colorless state, where the magenta ECP is oxidized and the MCCP layer is neutralized, is more detrimental to device stability than driving the device into the colored state.

To effectively drive electrochromic devices as a clock, asymmetric switching of the device must be stable both during prolonged segment switching in the colored state as well as in the colorless state. As mentioned previously, decreasing the voltage window is expected to improve the device lifetime. To assess whether this strategy would prolong the lifetime of devices switched under the most unfavorable asymmetrical conditions (3.3 s magenta, 6.6 s transparent), we employed lowered voltages of +0.6 and −0.3 V and the device was switched for more than 100 000 cycles. In these devices, deterioration does occur, again, especially for smaller elements, but the device performance is otherwise comparable to the previously presented device switched asymmetrically with prolonged application of a negative voltage. Although the reduced voltage slows down the switching speed from the magenta to the transparent state to around 4 s, applying a narrower voltage window allows for stable asymmetric device operation over at least 100 000 cycles (see Figure S4a−d in the Supporting Information).

3. CONCLUSION

In this study, we have demonstrated the use of SU-8 wells to simultaneously offer individual ECP cells as well as to optimize electrolyte layer thickness in electrochromic devices. Moreover, the deposition of the ECP, counter electrode, and electrolyte, as well as the lamination and UV curing/sealing of the device, were all performed under ambient conditions. This device architecture, combined with the inherently stable polymers used, afforded rapid segment switching within a narrow voltage window as well as exceptional long-term stability over 200 000 cycles. We addressed unique challenges encountered while operating the device as a clock using a PCB, where asymmetric switching leads to more rapid device failure than observed in symmetrically switched devices. By using narrower voltage windows, the device switching speeds were slightly slower, whereas the stability was greatly improved. These results offer an attractive outlook on the performance, stability, and processability of electrochromic devices, while outlining some of the novel challenges ahead as these devices become more sophisticated.

4. EXPERIMENTAL SECTION

Polymers. PProDOT-$(CH_2OEtHx)_2$ was used as the ECP on the active layer and synthesized according to a previously reported procedure.[22] The ECP's M_w is about 13 kDa and the sprayed layer's thickness is in the range of 200−250 nm. A PProDOP minimally color changing polymer (MCCP) was used as the charge collecting layer on the counter electrode, and was also synthesized according to a previously reported procedure.[4] The MCCP has an M_w value of around 60 kDa and the sprayed layer's thickness is around 150−200 nm.

Electrolyte. A faint-yellow UV-curable electrolyte was formulated consisting of 0.5 M $LiCF_3SO_3$ in propylene carbonate (PC) with 3-wt % PMMA (M_w = 996 000 g/mol) as a thickener and additional cross-linking agents (26-wt % monomer 1,6-hexanediol diacrylate (HDODA) cross-linked with 6-wt % Irgacure 2022 and 0.5-wt % Irgacure 184). Cross-linking agents, monomers and additional polymers for the UV-curable electrolyte were provided by BASF.

Well Material. The well material (SU-8) was purchased from Microchem Corp.

Substrates. Glass substrates were purchased from Corning, ITO-coated polyether sulfone (PES) foil substrates from Sumitomo Bakelite.

Device Manufacture. The backplane consists of an ITO layer that is sputtered onto the glass substrate. Then, SU-8, which acts as encapsulation and spacer, is spin coated and structured lithographically. To pattern the ECP material a lift off process is used. Therefore, a negative tone photoresist (maN-1420 from micro resist technology GmbH) is applied via spray coating (pressure 1.5 bar, 0.4 mm nozzle) onto the substrates and structured by standard lithographic processes. After this, the ECP is deposited by spray coating from a toluene solution (pressure 1.5 bar, 0.2 mm nozzle). After the ECP layer is sufficiently dried, the substrates are immersed into an acetone ultrasonic bath and thereby the photoresist and the ECP are stripped (lift off process). Substrates are then baked at 80 °C for 30 min to remove residual solvent. The frontplane substrate serves as the device counter electrode, consisting of a PES foil coated with

DOI: 10.1021/acsami.5b02090
ACS Appl. Mater. Interfaces 2015, 7, 12001−12008

ITO, and an additional MCCP layer, deposited by spray coating from toluene, serving as a charge-storage layer. Afterward, the MCCP layer is electrochemically oxidized in a separate electrochemical cell setup prior to device assembly. After the fabrication of back- and frontplane, the 2-electrode electrochromic device is assembled using a simple lamination process. First, a line of the uncured electrolyte is deposited along one edge of the backplane. Starting at that edge, the flexible PES foil is then rolled onto the backplane and electrolyte with a laminator as depicted in Figure 1, thereby filling the electrolyte into the SU-8 wells, and sealing the device at the same time. A thin layer of residual electrolyte remains on top of the SU-8 layer, which serves as an adhesive between the two substrates after UV-curing for 1 min at approximately 8 mW/cm^2. Finally, a chemically resistant polymer adhesive is applied at the edges of the PES foil.

Instrumentation. A SpectraScan PR-650 from Photo Research was used for spectral transmission measurements. Cyclic voltammetry measurements were done by a Keithley 4200-SCS. Switching speeds were measured with a custom-made setup. A Wavetek model 295 was used to cycle the devices.

■ ASSOCIATED CONTENT

Ⓢ Supporting Information

Figures S1−S5 as described in the text (PDF); time lapse video of ECD clock display (MPG). The Supporting Information is available free of charge on the ACS Publications website at DOI: 10.1021/acsami.5b02090.

■ AUTHOR INFORMATION

Corresponding Author

*E-mail: igm@igm.uni-stuttgart.de.

Present Address

§D.E.S. is currently at School of Chemistry and Biochemistry, School of Materials Science and Engineering, Center for Organic Photonics and Electronics, Georgia Institute of Technology, Atlanta, GA, USA.

Author Contributions

The manuscript was written through contributions of all authors. All authors have given approval to the final version of the manuscript.

Notes

The authors declare no competing financial interest.

■ ACKNOWLEDGMENTS

The authors gratefully acknowledge Mr. Ilja Vladimirov for AFM measurments of MCCP slides and the German Ministry of Education and Research (BMBF) for financial support within the project KOSADIS (FKZ 13N10766) in the framework of the leading edge cluster “Forum Organic Electronics”.

■ REFERENCES

(1) Amb, C. M.; Dyer, A. L.; Reynolds, J. R. Navigating the Color Palette of Solution-Processable Electrochromic Polymers. *Chem. Mater.* **2011**, *23*, 397−415.

(2) Österholm, A. M.; Shen, D. E.; Kerszulis, J. A.; Bulloch, R. H.; Kuepfert, M.; Dyer, A. L.; Reynolds, J. R. Four Shades of Brown: Tuning of Electrochromic Polymer Blends Toward High-Contrast Eyewear. *ACS Appl. Mater. Interfaces* **2015**, *7*, 1413−1421.

(3) Bulloch, R. H.; Kerszulis, J. A.; Dyer, A. L.; Reynolds, J. R. An Electrochromic Painter's Palette: Color Mixing via Solution Co-Processing. *ACS Appl. Mater. Interfaces* **2015**, *7*, 1406−1412.

(4) Knott, E. P.; Craig, M. R.; Liu, D. Y.; Babiarz, J. E.; Dyer, A. L.; Reynolds, J. R. A Minimally Coloured Dioxypyrrole Polymer as a Counter Electrode Material in Polymeric Electrochromic Window Devices. *J. Mater. Chem.* **2012**, *22*, 4953−4962.

(5) Österholm, A. M.; Shen, D. E.; Dyer, A. L.; Reynolds, J. R. Optimization of PEDOT Films in Ionic Liquid Supercapacitors: Demonstration As a Power Source for Polymer Electrochromic Devices. *ACS Appl. Mater. Interfaces* **2013**, *5*, 13432−13440.

(6) Søndergaard, R. R.; Hösel, M.; Krebs, F. C. Roll-to-Roll Fabrication of Large Area Functional Organic Materials. *J. Polym. Sci., Part B: Polym. Phys.* **2013**, *51*, 16−34.

(7) Jensen, J.; Krebs, F. C. From the Bottom Up - Flexible Solid State Electrochromic Devices. *Adv. Mater.* **2014**, *26*, 7231−7234.

(8) Kim, Y.; Kim, H.; Graham, S.; Dyer, A.; Reynolds, J. R. Durable Polyisobutylene Edge Sealants for Organic Electronics and Electrochemical Devices. *Sol. Energy Mater. Sol. Cells* **2012**, *100*, 120−125.

(9) Jensen, J.; Madsen, M. V.; Krebs, F. C. Photochemical Stability of Electrochromic Polymers and Devices. *J. Mater. Chem. C* **2013**, *1*, 4826−4835.

(10) Zhu, Y.; Otley, M. T.; Alamer, F. A.; Kumar, A.; Zhang, X.; Mamangun, D. M. D.; Li, M.; Arden, B. G.; Sotzing, G. A. Electrochromic Properties as a Function of Electrolyte on the Performance of Electrochromic Devices Consisting of a Single-Layer Polymer. *Org. Electron.* **2014**, *15*, 1378−1386.

(11) Vlachopoulos, N.; Nissfolk, J.; Möller, M.; Briançon, A.; Corr, D.; Grave, C.; Leyland, N.; Mesmer, R.; Pichot, F.; Ryan, M.; Boschloo, G.; Hagfeldt, A. Electrochemical Aspects of Display Technology Based on Nanostructured Titanium Dioxide with Attached Viologen Chromophores. *Electrochim. Acta* **2008**, *53*, 4065−4071.

(12) Noh, C. H.; Lee, J. M.; Jeon, S. J.; Das, R. R.; Jin, Y. W.; Lee, S. Y.; Son, S. U.; Sharmoukh, W. New Electrochromic Systems having Controllable Color and Bistability. *Dig. Tech. Pap. - Soc. Inf. Disp. Int. Symp.* **2009**, *40*, 1508−1511.

(13) Berggren, M.; Forchheimer, R.; Bobacka, J.; Svensson, P.-O.; Nilsson, D.; Larsson, O.; Ivaska, A. In *Organic Semiconductors in Sensor Applications*; Bernards, D. A., Malliaras, G. G., Owens, R. M., Eds.; Springer: Berlin, 2008; Chapter 9, pp 263−280.

(14) Chung, D. S.; Kim, J. W.; Noh, C. H.; Kim, E. S.; Chun, Y. T.; Jeon, S. J.; Das, R. R.; Song, B. G.; Jin, Y. W.; Lee, S. Y. 4.8″ QVGA Electrochromic Displays Driven by Oxide TFTs. *Dig. Tech. Pap. - Soc. Inf. Disp. Int. Symp.* **2010**, *41*, 1640−1642.

(15) Yashiro, T.; Hirano, S.; Naijoh, Y.; Okada, Y.; Tsuji, K.; Abe, M.; Murakami, A.; Takahashi, H.; Fujimura, K.; Kondoh, H. Novel Design for Color Electrochromic Display. *Dig. Tech. Pap. - Soc. Inf. Disp. Int. Symp.* **2011**, *42*, 42−45.

(16) Kawahara, J.; Ersman, P. A.; Nilsson, D.; Katoh, K.; Nakata, Y.; Sandberg, M.; Nilsson, M.; Gustafsson, G.; Berggren, M. Flexible Active Matrix Addressed Displays Manufactured by Printing and Coating Techniques. *J. Polym. Sci., Part B: Polym. Phys.* **2013**, *51*, 265−271.

(17) Shim, G. H.; Han, M. G.; Sharp-Norton, J. C.; Creager, S. E.; Foulger, S. H. Inkjet-Printed Electrochromic Devices Utilizing Polyaniline−Silica and Poly(3,4-Ethylenedioxythiophene)−Silica Colloidal Composite Particles. *J. Mater. Chem.* **2008**, *18*, 594−601.

(18) Kim, S. H.; Hong, K.; Lee, K. H.; Frisbie, C. D. Performance and Stability of Aerosol-Jet-Printed Electrolyte-Gated Transistors Based on Poly(3-hexylthiophene). *ACS Appl. Mater. Interfaces* **2013**, *5*, 6580−6585.

(19) Vasilyeva, S. V.; Beaujuge, P. M.; Wang, S.; Babiarz, J. E.; Ballarotto, V. W.; Reynolds, J. R. Material Strategies for Black-to-Transmissive Window-Type Polymer Electrochromic Devices. *ACS Appl. Mater. Interfaces* **2011**, *3*, 1022−1032.

(20) Berggren, M.; Nilsson, D.; Robinson, N. D. Organic Materials for Printed Electronics. *Nat. Mater.* **2007**, *6*, 3−5.

(21) Argun, A. A.; Aubert, P.-H.; Thompson, B. C.; Schwendeman, I.; Gaupp, C. L.; Hwang, J.; Pinto, N. J.; Tanner, D. B.; MacDiarmid, A. G.; Reynolds, J. R. Multicolored Electrochromism in Polymers: Structures and Devices. *Chem. Mater.* **2004**, *16*, 4401−4412.

(22) Reeves, B. D.; Grenier, C. R. G.; Argun, A. A.; Cirpan, A.; McCarley, T. D.; Reynolds, J. R. Spray Coatable Electrochromic Dioxythiophene Polymers with High Coloration Efficiencies. *Macromolecules* **2004**, *37*, 7559−7569.

DOI: 10.1021/acsami.5b02090
ACS Appl. Mater. Interfaces 2015, 7, 12001−12008

(23) Vasilyeva, S. V.; Unur, E.; Walczak, R. M.; Donoghue, E. P.; Rinzler, A. G.; Reynolds, J. R. Color Purity in Polymer Electrochromic Window Devices on Indium−Tin Oxide and Single-Walled Carbon Nanotube Electrodes. *ACS Appl. Mater. Interfaces* **2009**, *1*, 2288−2297.
(24) Lu, W.; Fadeev, A. G.; Qi, B.; Smela, E.; Mattes, B. R.; Ding, J.; Spinks, G. M.; Mazurkiewicz, J.; Zhou, D.; Wallace, G. G.; MacFarlane, D. R.; Forsyth, S. A.; Forsyth, M. Use of Ionic Liquids for π-Conjugated Polymer Electrochemical Devices. *Science* **2002**, *297*, 983−987.
(25) Jensen, J.; Dam, H. F.; Reynolds, J. R.; Dyer, A. L.; Krebs, F. C. Manufacture and Demonstration of Organic Photovoltaic-Powered Electrochromic Displays Using Roll Coating Methods and Printable Electrolytes. *J. Polym. Sci., Part B: Polym. Phys.* **2012**, *50*, 536−545.
(26) Kumar, A.; Otley, M. T.; Alamar, F. A.; Zhu, Y.; Arden, B. G.; Sotzing, G. A. Solid-State Electrochromic Devices: Relationship of Contrast as a Function of Device Preparation Parameters. *J. Mater. Chem. C* **2014**, *2*, 2510−2516.
(27) Alamer, F. A.; Otley, M. T.; Zhu, Y.; Kumar, A.; Sotzing, G. A. Dependency of Polyelectrolyte Solvent Composition on Electrochromic Photopic Contrast. *Sol. Energy Mater. Sol. Cells* **2015**, *132*, 131−135.
(28) Padilla, J.; Seshadri, V.; Otero, T. F.; Sotzing, G. A. Electrochemical Study of Dual Conjugated Polymer Electrochromic Devices. *J. Electroanal. Chem.* **2007**, *609*, 75−84.

DOI: 10.1021/acsami.5b02090
ACS Appl. Mater. Interfaces 2015, 7, 12001−12008